Environmental and Climate Technologies
2024, vol. 28, no. 1, pp. 724–737
https://doi.org/10.2478/rtuect-2024-0056
https://content.sciendo.com

Study of the Influence of Temperature and Pressure on the Intensity of Gas Hydrate Formation

Anatoliy PAVLENKO*

Kielce University of Technology, aleja Tysiąclecia Państwa Polskiego, 7, 25-314, Kielce, Poland

Received 21.10.2024; accepted 03.11.2024

***Abstract* – The paper analyses the influence of pressure and temperature of gas and liquid on the process of hydrate formation, proposes equations that allow to predict the course of heat and mass exchange processes of gas hydrate synthesis and estimate the amount of gas hydrate obtained at given thermodynamic parameters. The synthesis of gas hydrates begins with the creation of appropriate thermodynamic conditions in the reactor. However, the formation of hydrate layers on the surfaces of gas bubbles in bubbling or high-speed mixing technologies has peculiarities associated with the fact that the temperature and pressure of the gas change depending on the bubble size fluctuations. This should be taken into account when determining the conditions of hydrate formation. To this end, the article proposes a mathematical model that allows the thermodynamic conditions of synthesis to be optimised. The obtained results can be used to design process equipment and optimise its parameters.**

***Keywords* – Gas hydrates; gas pressure; gas temperature; phase changes.**

1. INTRODUCTION

In many countries worldwide, gas hydrates are considered one of the most promising alternative energy sources. Global gas hydrate reserves are estimated to be at least 250 trillion m^3 [1]–[3]. This exceeds the known reserves of conventional natural gas, which, according to current data, amount to 187.1 trillion m^3 [4], [5].

A key advantage of gas hydrates for storage and transport is their ability to self-preserve, allowing for storage and transport at atmospheric pressure [6], [7]. Synthesized gas hydrates enable the transport and storage of light hydrocarbons (methane, ethane), which are often flared at production sites, significantly contributing to environmental pollution in surrounding areas [8].

The main thermodynamic parameters that determine the stability of hydrates are pressure and temperature. The behaviour of hydrates under pressure varies from destabilisation of KS-II hydrates with a stoichiometric composition of 1:17 (e.g., for $THF{\cdot}17H_2O$ hydrates, $dT/dP = 2.5$ K/kbar, $k = 0.485$) to significant stabilisation for KS-I hydrates (e.g., for $C_2H_4O{\cdot}6.7H_2O$, $dT/dP = 7.0$ K/kbar, $k = 0.537$) [9], [10]. A characteristic feature of crystalline hydrates is that their formation temperature is much higher than the freezing point of water. However, as the temperature increases, the pressure must be increased to form a gas hydrate. Above this temperature, methane hydrate is formed only at very high pressures, and other gases liquefy during compression [11]–[14], see Table 1.

* Corresponding author.
E-mail address: apavlenko@tu.kielce.pl

TABLE 1. CRITICAL TEMPERATURES OF NATURAL GAS HYDRATE FORMATION

Hydrocarbon gases	**Ethane**	**Methane**	**Isobutane**	**Propane**
Temperature, °C	14.5	23	2.5	5.5
Pressure, bar	35	300	1.7	5.5

This implies that hydrates will inevitably form within this stability domain, provided sufficient gas and water are present. At exceedingly high pressures, the volumetric equivalence of the hydrate phase and its decomposition products results in a maximum in the hydrate decomposition curve (lhg), occurring at 47.7 °C and 500 MPa.

At point Q_h, a discontinuity in the hydrate decomposition curve is observed, attributed to the formation of a new hydrate, h_x, whose composition and structure remain undetermined. The inclusion of guest molecules within the clathrate water lattice results in an increased packing coefficient compared to ice Ih ($k = 0.43$), reaching 0.47–0.52 for structure KS II hydrates (with a stoichiometric composition of 1:17), 0.53–0.58 for structure KS I hydrates, and 0.59–0.60 for fully occupied hydrates. The behaviour of hydrates under pressure varies from decomposition to varying degrees of stabilization. Even in the best-case scenario, the complementarity between the guest molecule and the host cavity is insufficient to form a denser packing with a coefficient approaching 0.74. Consequently, at high pressures, the density of the clathrate structure becomes lower than that of the gas phase, leading to maxima in the hydrate decomposition curves [15].

Studies [16], and [17] highlight that even under favourable thermodynamic conditions, hydrate formation often requires significant time. While hydrate decomposition generally occurs more readily, hydrocarbon hydrates at temperatures below 0 °C and relatively low pressures are metastable. These hydrates decompose gradually and can persist for years due to a self-preservation effect [18]. According to several researchers, this effect is attributed to the formation of an ice crust upon decomposition, which prevents further breakdown. This crucial property is well-documented in studies [19], [20]. Thus, while phase diagrams delineate the stability regions of gas hydrates, they do not provide information regarding the kinetics of hydrate formation or dissociation. Further investigations are required to determine these characteristics.

2. KINETICS OF HYDRATE FORMATION

The first studies of hydrate formation kinetics are presented in [21]. The studies were carried out to determine the composition of hydrates and to obtain hydrates of various gases. However, the issue of improving the technology of hydrate production was not relevant at that time, and the purpose of the research was usually to prevent hydrate formation in wells and gas pipelines. Further studies [22]–[26] were devoted to the study of cyclic processes of hydrate synthesis and dissociation, and they also evaluated gas diffusion through hydrate. The authors showed the possibility of synthesising small amounts of gas hydrates in the laboratory over a long period of time. Recently, due to the need for industrial use of GH, there has been a need to improve the technologies for their synthesis. Studies [27] have shown a very weak dependence of the hydrate formation kinetics on the temperature of the reactor environment, and gas pressure was determined as the main driving force of the hydrate formation process. In study [28], it is noted that the growth rate of the hydrate film is proportional to the temperature difference between the equilibrium state of the hydrate at the operating pressure and the gas temperature (supercooling). In work [29], the kinetics of hydrate film growth is based on the heat transfer of the interfacial surface with the surrounding environment. The

thickness of the hydrate film on the interfacial surface was investigated in [30] using a laser interferometer. It was established that within 150 hours it reaches 40 μm. Additionally, research into methods of intensifying gas hydrate synthesis has become increasingly active. In particular, works [31]–[33] consider the influence of surfactants on the rate of hydrate formation. In article [34], a mathematical model is proposed to determine the formation time of a hydrate film on the interfacial surface depending on the gas pressure and the number of nucleation sites. It is known that the rate of hydrate formation can vary widely, from practically two weeks to several minutes. To improve the technology of gas hydrate synthesis, studies on the influence of various factors on this process are essential. Laboratory studies [35] show that hydrate formation under isochoric-isothermal conditions (static mode) takes a long time – from six hours to several weeks. According to [36], the kinetics of methane hydrate formation is described by the function

$$U = U_{\text{o}} - \frac{U_{\text{o}}}{e^{kt}}\ , \tag{1}$$

where U_{o} – calculated amount of hydrate, m^3; k – hydrate formation rate constant, s^{-1}; t – time of the hydrate formation process, s. This dependence reflects only the general nature of the hydrate formation process in time.

Study [37] reveals that supercooling by 1–2 °C markedly enhances hydrate formation rates, although further supercooling leads to a gradual decrease in hydrate crystal growth, deviating from the predictions of Eq. (1). Article [38] examines gas hydrate formation under both free and forced mixing conditions, as well as in the presence of a constant magnetic field. The authors' choice of hydrate formation time as a parameter does not provide a direct measure of mass transfer rates. While [39] proposes using a water injector to accelerate hydrate formation, quantitative data on mass transfer rates are absent. The kinetics equation for the formation of refrigerant R12 (CF2Cl2) hydrate is derived in [40].

$$r = 0.4\Delta T^{0.5}\omega^{0.288}t^{-0.45}\ , \tag{2}$$

where r is the hydrate formation rate (kg $H_2O/m^3 \cdot s$), ΔT is the temperature difference, and ω is the mass ratio of hydrate-forming agent in the crystallizer.

An analysis of the graphical data presented in this study clearly indicates that the rate of hydrate formation is primarily dependent on time. The influence of other factors falls within the experimental error. Depending on the process conditions, [41]–[45] systematizes five models for hydrate formation kinetics: at the surface of bubbles, growth of a hydrate film on a stationary water surface, with the use of stirrers, based on mass transfer processes, and the growth of hydrate crystals from ice. Empirical coefficients in the equations are provided only for methane and ethane. An analysis of the aforementioned studies reveals the empirical nature of the obtained dependencies, which require adjustments under different hydrate formation conditions. The influence of gas pressure, liquid temperature, bubble size, types of surfactants, and other factors on this process has been insufficiently studied. The lack of such critical information significantly complicates the decision-making process in the design of industrial installations for hydrate synthesis

3. Model of Gas Hydrate Formation on the Surface of Gas Bubbles

The Rayleigh-Plesset equation, as presented in [46] and [47], serves as the foundation for modeling the hydrate formation process. This equation describes the behaviour of a bubble as it transitions to a new state of thermodynamic equilibrium:

$$\frac{\rho}{4}\left[D\frac{\mathrm{d}^2 D}{\mathrm{d}t^2}+3\left(\frac{\mathrm{d}D}{\mathrm{d}t}\right)^2\right] = P_\mathrm{b}-P-\frac{\sigma}{D}-\frac{4\mu}{D}\frac{\mathrm{d}D}{\mathrm{d}t}, \tag{3}$$

where D is the diameter of the gas bubble (m), t is time (s), μ is the dynamic viscosity of the liquid (Pa·s), σ is the surface tension of the liquid (N/m), ρ is the density of the liquid (kg/m³), P_b is the pressure inside the bubble (Pa), and P is the pressure in the liquid at a distance from the bubble (Pa). The velocity of the liquid ($v = \mathrm{d}D/(2\mathrm{d}t)$) at the bubble boundary can be determined by integrating Eq. (3):

$$\frac{\mathrm{d}v}{\mathrm{d}t}=\frac{2\left(P_\mathrm{b}-P\right)}{\rho D}-3\frac{v^2}{D}-\frac{16\mu v}{\rho D^2}-\frac{8\sigma}{\rho D^2}. \tag{4}$$

At the initial time, a bubble with diameter D and internal pressure P_b appears in a liquid with pressure P. If the bubble is in equilibrium with the liquid, then from Eq. (4), subject to the condition $0.5\mathrm{d}D/\mathrm{d}t$, we obtain

$$P_\mathrm{b}=P+\frac{4\sigma}{D}. \tag{5}$$

If the mass of gas in the bubble changes as a result of mass transfer processes on its surface, then

$$\frac{\mathrm{d}\rho}{\mathrm{d}t}=\frac{6}{D}\left\{ I-\rho\frac{\mathrm{d}D}{2\mathrm{d}t}\right\}, \tag{6}$$

where I is the mass of gas entering the gas space of the bubble or diffusing into the liquid and forming a hydrate layer through a unit area per unit time, kg/(m²s). It follows from Eq. (6) that the density of the gas in the bubble changes significantly due to the mass transfer with the interfacial surface of the bubble.

The first law of thermodynamics is used to determine the temperature inside the bubble. For a mixture of gas and vapour, it can be written as follows:

$$\frac{\mathrm{d}\left[m_\mathrm{g}c_\mathrm{g}+m_\mathrm{i}c_\mathrm{i}\right]T}{\mathrm{d}t}=\pi D^2 q-P_\mathrm{b}\pi\frac{\mathrm{d}D^3}{6\mathrm{d}t}, \tag{7}$$

where m_g, m_i are the masses of gas and vapour, kg; c_g, c_i are the heat capacities of gas and vapour, J/(kg·°C); q is the specific heat flux at the bubble surface, W/m².

From this equation, we obtain:

$$\frac{\mathrm{d}T}{\mathrm{d}\tau}=\frac{3\left(q-T\left(c_\mathrm{i}I_\mathrm{i}+c_\mathrm{p}I_\mathrm{p}\right)-\frac{T\left(c_\mathrm{i}I_\mathrm{ip}+c_\mathrm{p}I_\mathrm{pv}\right)R}{3}-P_\mathrm{b}\frac{\mathrm{d}R}{\mathrm{d}\tau}\right)}{R\left(c_\mathrm{i}I_\mathrm{i}+c_\mathrm{p}I_\mathrm{p}\right)}. \tag{8}$$

Eq. (8) includes several unknown variables: specific heat flux (q), specific surface mass flux of gas (I_g) and vapour (I_i), and specific volumetric mass fluxes of gas (I_{gv}) and vapour (I_{iv}). A temperature difference between the vapour bubble wall and the gas-vapour mixture inside it is a prerequisite for the emergence of heat flux. The driving force for mass transfer fluxes is the difference in partial pressures near the vapour bubble wall and its internal environment. The component $T(c_gI_g+c_iI_i)$ represents the heat fluxes supplied to the bubble wall due to mass transfer processes. Simultaneously, this heat flux is lost to the gas-vapour environment of the bubble. The equations presented above allow us to describe the process of gas bubble oscillations. However, the intense exchange of energy and mass between the bubble's internal environment and its interfacial surface can lead to rapid damping of oscillations

4. HEAT AND MASS TRANSFER AT THE INTERFACIAL SURFACE

The total specific heat flux (q) near the bubble surface consists of the following components:

– heat flux from molecules moving from the vapour-gas mixture to the bubble wall (q_1, q_2);
– heat flux from gas molecules that have rebounded from the bubble wall, evaporated from it, and are moving into the bubble (q_3, q_4);
– heat flux entering the bubble wall from its vapour-gas environment with vapour and gas molecules that condense on this surface (q_5, q_6) – as per Eq. (8).

The heat balance equation for these fluxes can be written as follows:

$$q = q_2 - q_1 + q_3 + q_4 - q_5 - q_6 , \tag{9}$$

where q_1,q_2,q_3,q_4 are the specific heat fluxes transferred by elastic collision of gas and vapour molecules with the bubble wall; q_5,q_6 are the specific heat fluxes transferred by mass transfer processes near the bubble surface.

Since the temperature of the gas in the bubble does not depend on the coordinate, and the temperature of the liquid surface is different from the gas temperature, there will be a temperature 'jump' between them. The heat flux transferred with the vapour molecules to the bubble surface can be calculated by the formula:

$$q_1 = I_i c_i T , \tag{10}$$

where I_i is the mass flux of vapour molecules to the liquid surface, kg/(m^2·s).

The thickness of the layer of gas molecules in the bubble participating in the processes at the liquid surface is equal to the free path length of the molecule. For bubbles filled with gas, especially under overpressure, the free path length of molecules is several orders of magnitude smaller than the bubble radius. Therefore, when considering heat and mass flows near the bubble surface, we will neglect its curvature.

$$q_1 = \frac{\rho_i v_i c_i T}{6} . \tag{11}$$

Similarly, the heat flux transferred by the gas molecules to the bubble surface can be found:

$$q_2 = \frac{\rho_g v_g c_g T}{6}, \tag{12}$$

where $v_g = \left(\frac{8 R_\mu T}{\mu_g \pi} \right)$ is the arithmetic mean velocity of the thermal motion of the gas molecules, m/s.

The heat flux entering the bubble with the vapour molecules reflected from the bubble wall,

$$q_3 = \frac{\rho_i v_i c_i T}{6} + I_i c_i T . \tag{13}$$

The heat flux entering the bubble with the „reflected" gas molecules,

$$q_4 = \frac{\rho_g v_g c_g T}{6} + I_g c_g T . \tag{14}$$

Heat flux with vapour molecules 'captured' by the liquid surface,

$$q_5 = I_i c_i T . \tag{15}$$

Heat flow with gas molecules 'captured' by the liquid surface,

$$q_6 = I_g c_g T . \tag{16}$$

To obtain the total heat flux, we substitute all the heat flux values into Eq. (9) and, assuming that the temperature difference between the gas and the bubble surface is within a few degrees, we can assume that the heat capacities are constant over a relatively small temperature range. The equation can then be rewritten as:

$$q = \left\{ \left(\frac{\rho_i v_i T}{6} + I_i \right) c_i + \left(\frac{\rho_g v_g T}{6} + I_g \right) c_g \right\} \left[T(\tau) - T \right] . \tag{17}$$

The heat balance equation must be supplemented by the mass balance equations for gas and vapour at the bubble surface. The driving force for the mass fluxes I_g, I_i is the difference in partial pressures or concentrations. To determine the mass flux, we use Fick's first law, according to which (the mass dm moving over an elementary surface dS in a time dt is proportional to the concentration gradient dc/dx of this substance).

$$\frac{\mathrm{d}m}{\mathrm{d}t} = -\Psi \mathrm{d}S \frac{\mathrm{d}C}{\mathrm{d}x}, \tag{18}$$

where Ψ is the mass diffusivity in m²/s. Considering a steady-state mass flux through a known area S, we can write the mass flow rate in kg/s as:

$$G_g = 4\pi\Psi R c_g . \tag{19}$$

Dividing by the surface area of the bubble gives the specific mass flux in the hydrate formation processes on the surface of the gas bubble

$$I_g = \frac{\Psi c_g}{R}. \tag{20}$$

It follows from the equation that the specific mass flux of gas diffusing into water decreases as the bubble size increases. Therefore, bubbles of a minimum size are required to intensify mass transfer processes

5. Influence of Thermodynamic Parameters on the Intensity of Gas Hydrate Formation

Various authors have experimentally investigated the influence of thermodynamic parameters on the rate of gas hydrate formation at the phase interface [44]–[48]. However, a comprehensive methodology for such an influence is still lacking. In order to solve this problem, the mathematical model of the hydrate formation process presented above is used in this paper, which includes the main thermodynamic parameters and the calculations obtained in comparison with experimental data.

It is known that thermodynamic conditions determine the range of existence of gas hydrates, so their influence is crucial. However, we are interested in quantitative parameters that influence the rate of gas hydrate formation. These parameters are:

- gas and liquid temperature;
- pressure in the liquid-gas system.

5.1. Influence of Gas Temperature

We will change the gas temperature from the start of hydrate formation to the freezing point of water on the surface of the methane bubble. The calculation results are shown in Fig. 2.

The blue line in Fig. 1 corresponds to a gas temperature of 6 °C, which is 0.5 °C higher than the hydrate formation temperature at this pressure. A further increase in temperature does not lead to hydrate formation within 200 μs, as the cooling of the gas in the bubble takes longer. In general, the hydrate formation process cannot begin until the temperature reaches 5.5 °C. The higher the initial gas temperature, the later the hydrate formation process starts.

The purple curve in Fig. 2 corresponds to an initial temperature that is 0.5 °C lower than the hydrate formation temperature. It can be seen that the hydrate formation process starts almost immediately and reaches its maximum values during the heating of the bubble. This amount of hydrate formed is normalized to 1.

The green curve in Fig. 1 corresponds to an initial gas temperature of 0 °C, which is 5.5 °C below the hydrate formation temperature. A sharp increase in hydrate quantity is evident. Quantitative analysis reveals a six-fold increase in hydrate formation.

At a gas temperature of −5°C (red curve in Fig. 1, 10.5 °C below the hydrate formation temperature), a significant (15-fold) increase in hydrate quantity is observed, while at −10 °C (blue curve, 15.5 °C below the hydrate formation temperature), a further, albeit less significant, increase is noted. This suggests that further cooling is ineffective. The reason for this is the hindered heat removal from the reaction zone. The freezing of inner layers and the sharp increase in thermal resistance between the gas and the hydrate formation zone impede heat transfer. The deterioration of heat removal slows down the hydrate formation process.

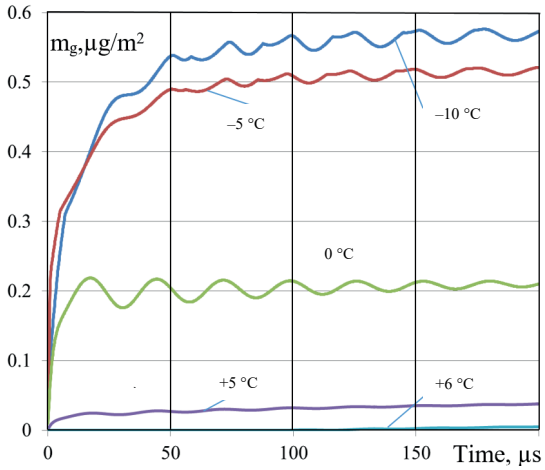

Fig.1. Influence of gas temperature on the hydrate formation process.

At an initial temperature of 6 °C, gradual cooling occurs until the hydrate formation temperature is reached. This cooling process is superimposed by a damped oscillatory process. Within 200 μs, the thermal wave penetrates 2.4 % of the bubble radius into the water. Hydrate formation commences only after sufficient cooling of the gas within the bubble. Under such conditions, the amount of hydrate formed is very small. When the initial gas temperature is lowered to 0 °C, the situation changes dramatically. The amount of hydrate formed increases significantly. However, hydrate formation occurs only in the first, thinnest layer of water, with a thickness of approximately 0.04 % of the bubble radius. Additionally, during oscillations, it may partially dissociate.

To induce hydrate formation in deeper liquid layers, the gas must be cooled. Mathematical modelling results indicate that the most significant oscillations (damped oscillations) of the bubble occur at the beginning of the hydrate formation process. The driving mechanism for these oscillations is the temperature difference between the vapour-gas environment of the bubble and the hydrate formation temperature, which is determined by the ambient pressure. During hydrate formation, a local increase in liquid temperature occurs, followed by an increase in the temperature of the vapour-gas environment of the bubble due to heat exchange. The increase in gas temperature leads to an increase in bubble pressure and initiates a process of increasing its diameter.

Thus, the maximum hydrate formation rate is observed during the period of gas heating in the bubble. This period is the most productive but has a short duration of 2–40 μs.

Over time, the oscillations damp out and the hydrate formation rate decreases. Gradually, in viscous fluids, the oscillations cease and the hydrate formation process is sustained by heat removal to the outer liquid layers.

5.2. Effect of Liquid Temperature on Hydrate Formation

Consider a methane bubble in water. The bubble diameter is 1 mm, and the initial gas temperature is 5 °C. The water temperature will be varied within the range of 0–5 °C. The calculated results for the bubble radius are presented in Fig. 2, where rapidly damping oscillations are observed, with amplitudes proportional to the decrease in water temperature. The radius varies within the range of 1–1.5 μm, which is 0.2–0.3 %.

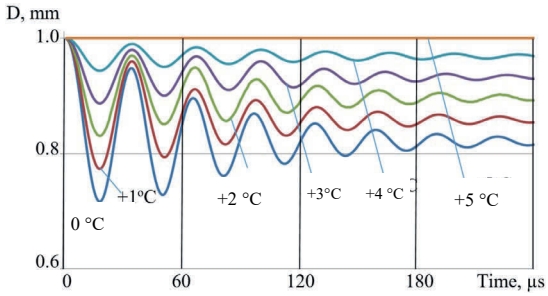

Fig. 2. Changes in the radius of a methane bubble in water at different temperatures.

Fig. 3 presents the vapour-gas phase pressure inside the bubble. Pressure oscillations are within the range of ±17 kPa (0.3 %). The temperature of the vapour-gas phase inside the bubble is shown in Fig. 4. A gradual cooling of the bubble to the hydrate formation temperature is observed. Moreover, the lower the water temperature, the higher the amplitude of the oscillations and the lower the gas temperature.

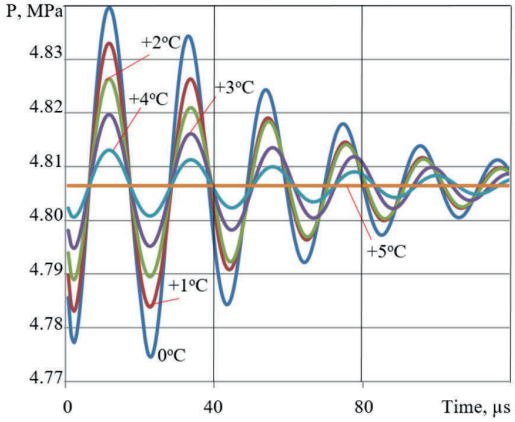

Fig. 3. Pressure of the vapour-gas medium inside the bubble as a function of water temperature.

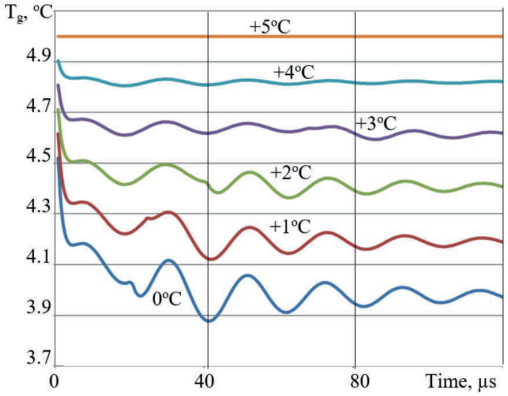

Fig. 4. Bubble gas temperature at different water temperatures.

The constant temperature at the bubble surface corresponds to the duration of hydrate formation in the boundary layer of the bubble. After filling this layer with hydrate, a damped oscillatory process near the hydrate formation temperature is observed. When the water temperature is decreased by 5 °C, the surface temperature decreases by only 1 °C, indicating the existence of reserves for intensifying hydrate synthesis. Such intensification can be achieved by increasing the pressure or reducing the initial temperature of the gas in the bubble.

The calculation results show that the rate of hydrate formation increases linearly in proportion to the decrease in water temperature. On the other hand, the rate of hydrate formation gradually decreases due to the deterioration of heat transfer between the hydrate formation area and the surrounding water layers. The increase in the thickness of the gas hydrate crust worsens the process of heat removal to the environment (water). Experimental data confirm this conclusion.

5.3. Influence of Gas Pressure on the Intensity of Hydrate Formation

The process of hydrate formation begins only when the gas pressure exceeds the minimum value characteristic of a given temperature. Gas pressure is a parameter that directly affects the efficiency of the gas hydrate synthesis process.

However, it is not clear how much more intensive the hydrate formation process will be when the pressure exceeds the equilibrium for the hydrate formation process at a given temperature. The results of mathematical modelling of hydrate formation at different methane pressures are shown in Fig. 5.

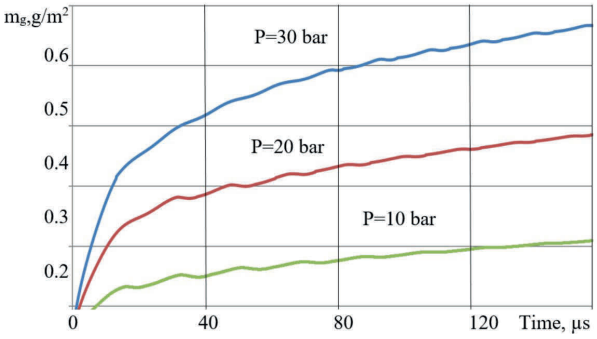

Fig. 5. Effect of gas pressure on methane hydrate formation.

Fig. 6 demonstrates that the amount of hydrate formed is proportional to the pressure in the gas-water system. Thus, the results of mathematical modelling show that increasing the pressure has a positive effect on the hydrate formation process.

5.4. Effect of Bubble-Size on the Intensity of the Hydrate Formation Process

For a bubble with an initial radius of 0.1 mm, the calculated results of its size and the mass of hydrate formed over time are shown in Fig. 6. The most intense hydrate formation coincides with the most intensive increase in bubble size. During the oscillatory process, the growth of the hydrate amount varies with periods of its dissociation. The growth phase coincides with the increase in bubble radius. After the damping of the oscillatory process, the bubble size stabilizes, but the hydrate continues to form due to heat removal to the liquid.

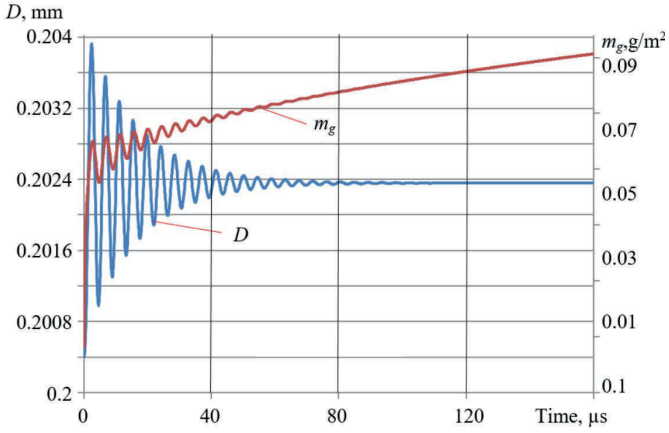

Fig. 6. Variation of bubble diameter (D) and specific mass of the formed hydrate (m_g).

Fig. 7 shows three characteristic temperature regions of the bubble: the heating region (from 0 °C to +7 °C), the damped oscillation region, and the stationary region. Small bubbles heat up very quickly, and this region is almost imperceptible on the graph. The heating region becomes noticeable only for relatively large bubbles. Due to intensive heat removal, the highest hydrate formation rate is observed in this region, but it has a short duration, and therefore the amount of hydrate formed is small.

For all bubble sizes, under the given initial conditions, the amplitude of temperature oscillations of the vapour-gas mixture does not exceed 0.5 °C. The logarithmic decrement of damping for bubbles with a radius of 0.01 mm is 0.32; for bubbles with a radius of 0.05 mm – 0.26; for bubbles with a radius of 0.1 mm – 0.25. After the completion of the oscillatory process, the temperature of the vapour-gas medium of the bubble practically does not change.

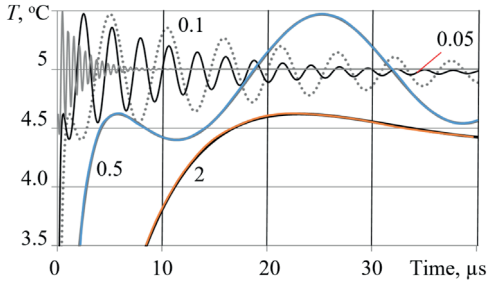

Fig. 7. Temperature of the vapour-gas medium of bubbles: 0.05 mm, 0.1 mm, 0.5 mm, 2 mm – bubble radius.

6. DISCUSSION

The analysis of the obtained dependencies indicates a significant influence of two factors on the hydrate formation rate: bubble size and time. For large bubbles (radius greater than 0.5 mm), the initial bubble heating stage has a dominant influence on hydrate formation. Subsequent bubble oscillations have little effect on the amount of hydrate formed. The small total surface area of such bubbles also does not contribute to an increase in the amount of hydrate. Medium-sized bubbles (with a radius of 0.1–0.05 mm) have two characteristic hydrate formation regions: the initial heating region and the heat exchange region with the

surrounding medium. Due to heat removal to water, the amount of hydrate formed gradually increases. The highest hydrate formation rate is characteristic of small bubbles (with a radius of 0.01 mm and less). The initial heating stage is very short here and does not play a significant role. The main amount of hydrate is formed in the process of heat exchange between the gas and the aqueous medium. Bubbles with a diameter greater than 1 mm have approximately the same hydrate formation rate. It is precisely such bubbles that are easiest to obtain under bubbling conditions. With a decrease in bubble size to less than 1 mm, the hydrate formation rate increases. This is especially noticeable for bubbles with a diameter of less than 0.02 mm. However, their production requires complex dispersers and additional energy costs. The maximum rate of gas hydrate formation is observed at the initial stage of bubble heating. This is typical for non-isothermal initial conditions. In large bubbles (radius greater than 2 mm), the oscillatory parameters have a dominant influence on hydrate formation. Their oscillations decay relatively slowly, and during this time, the main part of the hydrate is formed. However, large bubbles have a small total surface area of the phase contact. In general, an increase in bubble size leads to an increase in the thickness of the layer in which hydrate formation occurs. For large bubbles, the possibility of dissociation of part of the formed hydrate during the oscillation process is characteristic. For small bubbles, the hydrate continues to form during the entire time interval. For large bubbles, most of the hydrate is formed in the region of heating the gas medium of the bubble. Since the initial conditions are isothermal, the initial heating occurs due to hydrate formation.

7. CONCLUSION

This research investigates the impact of various factors on the thermodynamic state of an oscillating gas-vapour bubble and the associated mass transfer processes at the interface. The study reveals that initial temperature differences between the bubble's internal environment and the hydrate formation temperature drive oscillatory behaviour. During hydrate formation, local temperature increases and heat exchange between the bubble and its surroundings influence the bubble's diameter and the rate of hydrate formation. Each bubble size exhibits unique oscillation frequencies, and over time, oscillations damp down, leading to a stabilized hydrate formation process driven by heat dissipation. The initial heating phase of the gas within the bubble is characterized by the highest hydrate formation rates, although this rate gradually decreases. This study provides valuable insights into the complex dynamics of hydrate formation. The findings highlight the importance of controlling temperature, pressure, and bubble size to optimize hydrate production. Future research will focus on developing more accurate models and exploring additional factors that may influence hydrate formation. Thus, the synthesis of gas hydrates on the surface of gas bubbles has a complex dependence on gas pressure and temperature and, most importantly, these parameters are constantly changing with fluctuations in bubble size. These phenomena are inherent in the operation of bubbling devices, high-speed stirrers, etc. Therefore, in such technologies, it is necessary to determine the intervals of gas temperature and pressure in which the synthesis of gas hydrate would be sufficiently intensive.

REFERENCES

[1] Milkov A. V. Global estimates of hydrate-bound gas in marine sediments: how much is really out there? *Earth-Science Reviews* 2004:66(3–4):183–197. https://doi.org/10.1016/j.earscirev.2003.11.002

[2] Pavlenko A. M. Thermodynamic Features of the Intensive Formation of Hydrocarbon Hydrates. *Energies* 2020:13(13):3396. https://doi.org/10.3390/en13133396

[3] Pavlenko A., Koshlak H. A New Method for the Rapid Synthesis of Gas Hydrates for their Storage and Transportation. *Environmental and Climate Technologies* 2022:26(1):199–212. https://doi.org/10.2478/rtuect-2022-0016

[4] Pavlenko A. Application of Synthesized Hydrates in the National Economy. *Environmental and Climate Technologies* 2024:28(1):149–164. https://doi.org/10.2478/rtuect-2024-0013

[5] Boswell R., Hancock S., Yamamoto K., Collett T., Pratap M., Lee S. Natural Gas Hydrates: Status of Potential as an Energy Resource. *Future Energy* 3rd ed.; Improved Sustainable and Clean Options for our Planet; Elsevier: Amsterdam, The Netherlands, 2020:111–131. https://doi.org/10.1016/B978-0-08-102886-5.00006-2

[6] Veluswamy H. P, Kumar A., Kumar R., Linga P. An innovative approach to enhance methane hydrate formation kinetics with leucine for energy storage application. *Applied Energy* 2017:188:190–199. https://doi.org/10.1016/j.apenergy.2016.12.002

[7] Veluswamy H. P., Kumar A., Seo Y., Lee J. D., Linga P. A review of solidified natural gas (SNG) technology for gas storage via clathrate hydrates. *Applied Energy* 2018:216:262–285. https://doi.org/10.1016/j.apenergy.2018.02.059

[8] Yu H., Chen C., Wang F. Kinetic Promotional Effect of Methane Hydrate Formation in the Presence of Leucine. *Energy & Fuels* 2024:38(10):8641–8648. https://doi.org/10.1021/acs.energyfuels.4c00183

[9] Sharma D., Sowjanya Y., Chari V. D., Prasad P. Methane storage in mixed hydrates with tetrahydrofuran. *Indian J Chem Technol.* 2014:21:114–119.

[10] Delahaye A., Fournaison L., Marinhas S., Chatti I., Petitet J. P., Dalmazzone D., Fürst W. Effect of THF on equilibrium pressure and dissociation enthalpy of CO_2 hydrates applied to secondary refrigeration. *Ind. Eng. Chem. Res.* 2006:45:391–397. https://doi.org/10.1021/ie050356p

[11] Pavlenko A. M., Koshlak H. Intensification of Gas Hydrate Formation Processes by Renewal of Interfacial Area between Phases. *Energies* 2021:14(18):5912. https://doi.org/10.3390/en14185912

[12] Kipyoung K., Youtaek K., Hokeun K. Recent advances in natural gas hydrate. Carriers for gas transportation. *Journal of Advanced Marine Engineering and Technology* 2014:38(5):589–601. https://doi.org/10.5916/jkosme.2014.38.5.589

[13] Filarsky F., Schmuck C., Schultz H. J. Development of a Surface-Active Coating for Promoted Gas Hydrate Formation. *Chem. Ing. Tech*. 2019:91(12):85–91. https://doi.org/10.3390/molecules26123615

[14] Brown T. D., Taylor C. E., Bernardo M. P. Rapid Gas Hydrate Formation Processes: Will They Work? *Energies* 2010:3(6):1154–1175. https://doi.org/10.3390/en3061154

[15] Wang C., Li X., Liang S., Li Q., Pang W., Zhao B., Chen G., Sun C. Modeling on effective thermal conductivity of hydrate-bearing sediments considering the shape of sediment particle. *Energy* 2023:285:129338. https://doi.org/10.1016/j.energy.2023.129338

[16] Cheng C., Wang F., Tian Y., Wu X., Zheng J., Zhang J., Li L., Yang P.; Zhao J. Review and prospects of hydrate cold storage technology. *Renew. Sustain. Energy Rev*. 2020:117:109492. https://doi.org/10.1016/j.rser.2019.109492

[17] Zhao J., Lv Q., Li Y., Yang M., Liu W., Yao L., Wang S., Zhang Y., Song Y. In-situ visual observation for the formation and dissociation of methane hydrates in porous media by magnetic resonance imaging. *Magn. Reson. Imaging* 2015:33(4):485–490. https://doi.org/10.1016/j.mri.2014.12.010

[18] Pavlenko A., Basok B. I. Kinetics of Water Evaporation from Emulsions. *Heat Transfer Research* 2005:36(5):425–430. https://doi.org/10.1615/HeatTransRes.v36.i5.100

[19] Chen B., Sun H., Li K., Wang D., Yang, M. Experimental Investigation of Natural Gas Hydrate Production Characteristics via Novel Combination Modes of Depressurization with Water Flow Erosion. *Fuel* 2016:252:295–303. https://doi.org/10.1016/j.fuel.2019.04.120

[20] Xu H., Kong W., Yang F. Decomposition characteristics of natural gas hydrates in hydraulic lifting pipelines. *Natural Gas Industry B* 2019:6(2):159–167. https://doi.org/10.1016/j.ngib.2018.07.005

[21] Veluswamy H. P., Hong Q. W., Linga P. Morphology study of methane hydrate formation and dissociation in the presence of amino acid. *Crystal Growth & Design* 2016:16:5932–5945. https://doi.org/10.1021/acs.cgd.6b00997

[22] Gnanendran N., Amin R. Modelling hydrate formation kinetics of a hydrate promoter – water – natural gas system in a semibatch spray reactor. *Chem. Eng. Sci*. 2004:59(18):3849–3863. https://doi.org/10.1016/j.ces.2004.06.009

[23] Veluswamy H. P., Kumar S., Kumar R., Rangsunvigit P., Linga P. Enhanced clathrate hydrate formation kinetics at near ambient temperatures and moderate pressures: Application to natural gas storage. *Fuel* 2016:182:907–919. https://doi.org/10.1016/j.fuel.2016.05.068

[24] Sowjanya Y., Prasad P. S. R. Formation kinetics & phase stability of double hydrates of C_4H_8O and CO_2/CH_4: A comparison with pure systems. *J. Nat. Gas Sci. Eng*. 2014:18:58–63. https://doi.org/10.1016/j.jngse.2014.02.001

[25] Veluswamy H. P., Wong A. J. H., Babu P., Kumar R., Kulprathipanja S., Rangsunvigit P., Linga P. Rapid methane hydrate formation to develop a cost effective large scale energy storage system. *Chem. Eng. J*. 2016:290:161–173. https://doi.org/10.1016/j.cej.2016.01.026

[26] Ke W., Svartaas T. M., Chen D. A review of gas hydrate nucleation theories and growth models. *Journal of Natural Gas Science and Engineering* 2019:61:169–196. https://doi.org/10.1016/j.jngse.2018.10.021

[27] Pavlenko A. Self-preservation Effect of Gas Hydrates. *Rocznik Ochrona Środowiska* 2021:23:346–355. https://doi.org/10.54740/ros.2021.023

[28] Kiran B. S., Sowjanya K., Prasad P. S., Yoon J. H. Experimental investigations on tetrahydrofuran-methanewater system: Rapid methane gas storage in hydrates. Oil Gas Sci. Technol. Rev. *IFP Energ. Nouv*. 2019:74(12). https://doi.org/10.2516/ogst/2018092

[29] Stern L. A., Circone S., Kirby S. H., Durham W. B. Temperature, pressure, and compositional effects on anomalous or "self" preservation of gas hydrates. *Canadian Journal of Physics* 2003:81(1–2):271–283. https://doi.org/10.1139/p03-018

[30] Kumar A., Bhattacharjee G., Kulkarni B. D., Kumar R. Role of Surfactants in Promoting Gas Hydrate Formation. *Industrial & Engineering Chemistry Research* 2015:54(49):12217–12232. https://doi.org/10.1021/acs.iecr.5b03476

[31] Luan H., Liu M., Shan Q., Jiang Y., Yan P., Du X. Experimental Study on the Effect of Mixed Thermodynamic Inhibitors with Different Concentrations on Natural Gas Hydrate Synthesis. *Energies* 2024:17(9):2078. https://doi.org/10.3390/en17092078

[32] Wei Y., Maeda N. Dry Water as a Promoter for Gas Hydrate Formation: A Review. *Molecules* 2023:28(9):3731. https://doi.org/10.3390/molecules28093731

[33] Pavlenko A., Koshlak H., Usenko B. Heat and mass transfer in fluidized layer. *Metallurgical and Mining Industry* 2014:6:96–100.

[34] Lan X., Chen J., Li D., Zheng J., Linga P. Gas storage via clathrate hydrates: Advances, challenges, and prospects. *Gas Science and Engineering* 2024:129:205388. https://doi.org/10.1016/j.jgsce.2024.205388

[35] Gambelli A. M. Introduction to natural gas hydrate formation and applications, Advances in Natural Gas: Formation, Processing, and Applications. *Natural Gas Hydrates* 2024:3:3–25. https://doi.org/10.1016/B978-0-443-19219-7.00016-3

[36] Kim K., Truong-Lam H. S., Lee J. D., Sa J.-H. Facilitating clathrate hydrates with extremely rapid and high gas uptake for chemical-free carbon capture and methane storage. *Energy* 2023:270:126902. https://doi.org/10.1016/j.energy.2023.126902

[37] Sun L., Sun H., Yuan C., Zhang L., Yang L., Ling Z., Zhao J., Song Y. Enhanced clathrate hydrate formation at ambient temperatures (287.2 K) and near atmospheric pressure (0.1 MPa): Application to solidified natural gas technology. *Chemical Engineering Journal* 2023:454:3:140325. https://doi.org/10.1016/j.cej.2022.140325

[38] Gambelli A. M., Rossi F., Cotana F. Gas Hydrates as High-Efficiency Storage System: Perspectives and Potentialities. *Energies* 2022:15(22):8728. https://doi.org/10.3390/en15228728

[39] Xie J., Meng Q., Jiang A., Chen D., Wang Y., Jiao W., Liu R. Characterization of gas hydrate generation in SDS-R141b compounding static system. *Energy Sources, Part A: Recovery, Utilization, and Environmental Effects* 2024:46(1): 6725–6742. https://doi.org/10.1080/15567036.2024.2354933

[40] Liu W., Wang L., Yang M., Song Y., Zhang L., Li Q., Chen Y., Experimental Study on the Methane Hydrate Formation from Ice Powders. *Energy Procedia* 2014:61:619–623. https://doi.org/10.1016/j.egypro.2014.11.1184

[41] Koshlak H. Synthesis of Zeolites from Coal Fly Ash Using Alkaline Fusion and Its Applications in Removing Heavy Metals. *Materials* 2023:16(13):4837. https://doi.org/10.3390/ma16134837

[42] Basok B., Davydenko B., Koshlak H., Novikov V. Free Convection and Heat Transfer in Porous Ground Massif during Ground Heat Exchanger Operation. *Materials* 2022:15(14):4843. https://doi.org/10.3390/ma15144843

[43] Englezos P. Phase equilibrium in canonical cubic structure I (sI) and II (sII) and hexagonal (sH) gas hydrate solid solutions. *Fluid Phase Equilibria* 2024:578:114005. https://doi.org/10.1016/j.fluid.2023.114005

[44] Javidani A. M., Abedi-Farizhendi S., Mohammadi A., Mohammadi A. H., Hassan H., Pahlavanzadeh H. Experimental study and kinetic modeling of R410a hydrate formation in presence of SDS, tween 20, and graphene oxide nanosheets with application in cold storage. *Journal of Molecular Liquids* 2020:304:112665. https://doi.org/10.1016/j.molliq.2020.112665

[45] Gambelli A. M., Rossi F. Thermodynamic and kinetic characterization of methane hydrate nucleation, growth and dissociation processes, according to the Labile Cluster Theory. *Chem. Eng. J.* 2021:425:130706. https://doi.org/10.1016/j.cej.2021.130706

[46] Pavlenko A. M., Basok B. I. Regularities of boiling-up of emulsified liquids. *Heat Transfer Research* 2005:36(5):419–424. https://doi.org/10.1615/HeatTransRes.v36.i5.90

[47] Pavlenko A., Koshlak H., Usenko B. The processes of heat and mass exchange in the vortex devices. *Metallurgical and Mining Industry* 2014:3:55–59.